FORUM GEOGRAFI
ISSN: 0852-0682 | E-ISSN: 2460-3945

HTTPS://JOURNALS.UMS.AC.ID/INDEX.PHP/FG/

Research article

Integration of Topography Map and Land Use Change Modeling for Sustainable Tourism Development in Merapi Volcano, Indonesia

Syamsul Bachri[1,*], Sandy Budi Wibowo[2], Sunardi[3], Franck Lavigne[4], Sumarmi[1], Mellinia Regina Heni Prastiwi[1], A Riyan Rahman Hakiki[5], Tabita May Hidiyah[1], Nanda Regita Cahyaning Putri[1]

[1] Department of Geography, Universitas Negeri Malang, Jl. Semarang 5, Malang 65145, Indonesia; [2] Department of Geographic Information Science, Universitas Gadjah Mada, Bulaksumur, Yogyakarta 0274-6492599, Indonesia; [3] Department of Biology, Universitas Padjajaran, Sumedang, Indonesia; [4] Physical Geography Laboratory, University of Paris 1 Pantheon Sorbonne, Paris, France; [5] Department of Geography Education, Universitas Lambung Mangkurat, Jl. Brigjend H. Hasan Basri, Kalimantan Selatan, Indonesia.

[*)] Correspondence: syamsul.bachri.fis@um.ac.id

Citation:

Bachri, S., Wibowo, S. B., Sunardi, Lavigne, F., Sumarmi, Prastiwi, M. R. H., Hakiki A. R., Hidiyah, T. M., Putri, N. R. C. (2026). Integration of Topography Map and Land Use Change Modeling for Sustainable Tourism Development in Merapi Volcano, Indonesia. Forum Geografi.40(2),178-196.

Article history:
Received 23 September 2025
Revised: 18 March 2026
Accepted: 23 March 2026
Published: 15 Mei 2026

Abstract

Indonesia, as the country with the highest number of active volcanoes worldwide, faces significant challenges from volcanic hazards. Mount Merapi, one of the most active volcanoes, is surrounded by intensive tourism and residential development, which increase the region's vulnerability. This study integrates DEMNAS-based topographic analysis and the Land Change Modeler (LCM) with the Multi-Layer Perceptron (MLP)–Markov Chain algorithm to examine land-use dynamics and risks to tourism in the Opak Oyo Watershed. Multi-temporal Landsat imagery (2004, 2014, 2024) was classified using the CART algorithm, achieving an overall accuracy of 94.5% and a Kappa coefficient of 0.928. The results show that between 2014 and 2024, the area of built-up land increased by 47.12 km², while that of forests declined by 127.76 km², indicating strong anthropogenic pressure. The validated LCM model projected that by 2034 built-up land will expand to 228.13 km², increasing by 46.04 km² (3.53%) compared to 2024, while agricultural land is predicted to decrease by 100.14 km² (–7.67%). Forest areas are projected to increase by 90.75 km² (6.95%), reflecting ecological rehabilitation scenarios. Tourism risk analysis shows that a significant number of tourism sites are located within KRB III (a high-risk zone), where projected building expansion overlaps with areas exposed to pyroclastic flows and lahar hazards. The findings highlight that integrating topographic constraints with predictive land-use modeling provides a robust spatial framework for sustainable tourism development in volcanic regions. The approach supports risk-informed zoning, environmentally sensitive land allocation, and long-term spatial planning strategies in Mount Merapi and other hazard-prone landscapes.

Keywords: Merapi Volcano; Topographic Mapping; Land Use Change; Land Change Modeler; Sustainable Tourism Development

1. Introduction

Globally, the intersection between tourism development and volcanic hazard risk has become an increasing concern, particularly in countries located along active tectonic belts such as the Pacific Ring of Fire (Kristianto *et al.,* 2024). The unique characteristics of volcanic landscapes have made many active volcanoes prominent tourist destinations (Alfama *et al.,* 2024). However, infrastructure expansion and intensified human activities in hazard-prone areas are often not adequately balanced with risk-based planning and mitigation strategies. This situation increases the exposure of local communities and visitors to eruption threats, while simultaneously intensifying environmental pressures and land-use change (Lessy *et al.,* 2024; Meredith *et al.,* 2025). Such challenges are faced by Indonesia, one of the countries with the highest number of active volcanoes in the world, where dynamic volcanic activity coincides with rapid spatial and economic development in surrounding areas.

Volcanic activity in Indonesia experienced a significant increase in 2024. Volcanoes that showed heightened activity included Anak Krakatau, Ili Lewotolok, Marapi, Merapi and Semeru (ESDM, 2024). Among these, Mount Merapi became the primary focus due to its high level of hazard; its eruptions have the potential to cause material losses and casualties (Bachri *et al.,* 2015; Rani & Khotimah, 2021; Rasidi *et al.,* 2023). The main hazards associated with Merapi's eruptions include pyroclastic flows (Hadmoko *et al.,* 2018; Kassouk *et al.,* 2014; Rani & Khotimah, 2021); and incandescent rock ejections, heavy ashfall, lava flows and toxic gases (Malawani *et al.,* 2021; Thouret *et al.,* 2022). Additionally, secondary impacts such as lava dome collapses, lahar floods and flash floods also pose serious threats (Andreastuti *et al.,* 2023; Cando-Jácome & Martínez-Graña, 2019; J. C. Thouret *et al.,* 2022).

Despite the high disaster risk, the area surrounding Mount Merapi has been developed into a center of economic and social activities, particularly in the tourism and residential sectors. This development has also contributed to an increase in the vulnerability of the region surrounding the

volcano (Mutiarni *et al.,* 2022; Septikasari & Ayriza, 2018). More than one million people reside on the slopes of Merapi, despite it being recognized as one of the most active and hazardous volcanoes in the world (Baxter *et al.,* 2017; Thouret *et al.,* 2000; Walter *et al.,* 2007). As the tourism sector around Mount Merapi continues to grow, there has been increasing conversion of land into built-up areas, including residential zones, tourism facilities and supporting infrastructure. Additionally, many areas that were previously agricultural land have been transformed into tourism zones, impacting the ecosystem balance and increasing environmental pressures (Krisanti *et al.,* 2024). If not properly managed, these changes could have negative consequences for environmental sustainability, such as an increased risk of erosion, ecosystem degradation, and declining water resource quality.

In this context, topographic mapping and predictive land-use change modeling play a crucial role in understanding how tourism development and land-use changes impact environmental conditions and disaster mitigation. Topographic mapping can assist in interpreting areas that have undergone morphological changes before and after eruptions, volcanic material deposition zones, and regions affected by lateral and vertical erosion due to volcanic processes (Puspita & Sudaryatno, 2013). This enables the identification of disaster-prone zones, the designation of protected areas, and the design of optimal evacuation routes. Predictive land-use change modeling is not only useful for assessing potential land degradation (Bachri *et al.,* 2024), but also serves as a tool for monitoring and urban planning, particularly in tourism areas (Rimba *et al.,* 2020). The Land Change Modeler (LCM) is a widely used technique for analyzing and predicting land-use and land-cover (LULC) changes (Dammag *et al.,* 2023; Hasan *et al.,* 2020; Leta *et al.,* 2021). The method allows for the integration of biological, physical and socio-economic factors that act as dominant drivers of land-use transformation (Barbosa de Souza *et al.,* 2023; Dammag *et al.,* 2023). LCM is designed to address the complexity of land-use changes and their management (Barbosa de Souza et al., 2023; Gontier *et al.,* 2010; Leta *et al.,* 2021).

Although previous studies of the Merapi region have addressed volcanic hazard assessment, geomorphological mapping, and land-use change analysis, these themes have generally been examined separately (Santosa & Sutikno, 2006; Sejati & Neritarani, 2024; Solikhin *et al.,* 2015). Hazard studies tend to emphasize physical processes and risk zonation, while land-use modeling research often focuses on urban expansion or environmental degradation, without explicitly incorporating high-resolution topographic constraints or tourism-driven spatial dynamics (Budiyanto, 2020; Nugraha *et al.,* 2019; Solikhin *et al.,* 2015). In particular, the integration of DEMNAS-based topographic analysis with predictive Land Change Modeler (LCM) simulations to evaluate tourism–hazard interactions within a sustainable tourism development framework remains limited. Previous research has not systematically combined elevation-derived parameters (e.g., slope, morphology and erosion susceptibility), future LULC projections, and tourism spatial growth patterns into a single spatial decision-support model.

Therefore, the novelty of this study lies in its integrated analytical approach. By combining DEMNAS-derived topographic data, LCM-based land-use projections, and tourism–hazard spatial overlay analysis, the research goes beyond descriptive hazard mapping or retrospective land-use assessment. It introduces a scenario-based framework capable of anticipating how tourism expansion may intersect with morphologically sensitive and hazard-prone areas. This approach not only assesses physical and geographical factors in tourism management, but also projects land tourism growth scenarios and their impacts on ecological balance and disaster mitigation. By integrating topographic data with the LULC model, the effects of volcanic eruptions and land-use changes, particularly in tourism areas, can be anticipated. This also contributes to the preservation of land ecosystems through sustainable environmental and tourism management, in alignment with the objectives set forth in the UN Sustainable Development Goals (SDGs).

2. Methods

2.1. Study Area

The study was conducted within the ecological boundary of the Opak Oyo Watershed (OOW) (Figure 1), which is administratively located in Bantul Regency, Sleman Regency, Gunungkidul Regency and Yogyakarta City, covering an area of approximately 1304.95 km^2. The boundaries of the catchment area were identified using data from the Ministry of Environment and Forestry. Topographically, the area extends from the upper volcanic slopes of Mount Merapi in the north to the karst-dominated landscapes of Gunungkidul in the south, with elevations ranging from approximately 50 m to over 2,900 m above sea level. Slope gradients vary considerably, from flat alluvial plains (<8%) in the downstream areas, to steep volcanic terrains (>40%) in the upstream zone.

Land cover within the watershed is heterogeneous, consisting of protected forest in the upper slopes, mixed agriculture and plantations in midstream areas, and expanding built-up zones in peri-urban and tourism corridors. Forested areas play a critical role in slope stabilization and sediment retention, while agricultural and tourism-driven land conversion has intensified spatial pressure in recent decades. These physical and environmental characteristics make the OOW a highly dynamic volcanic landscape, where geomorphological processes, hydrological dynamics, and tourism development interact simultaneously.

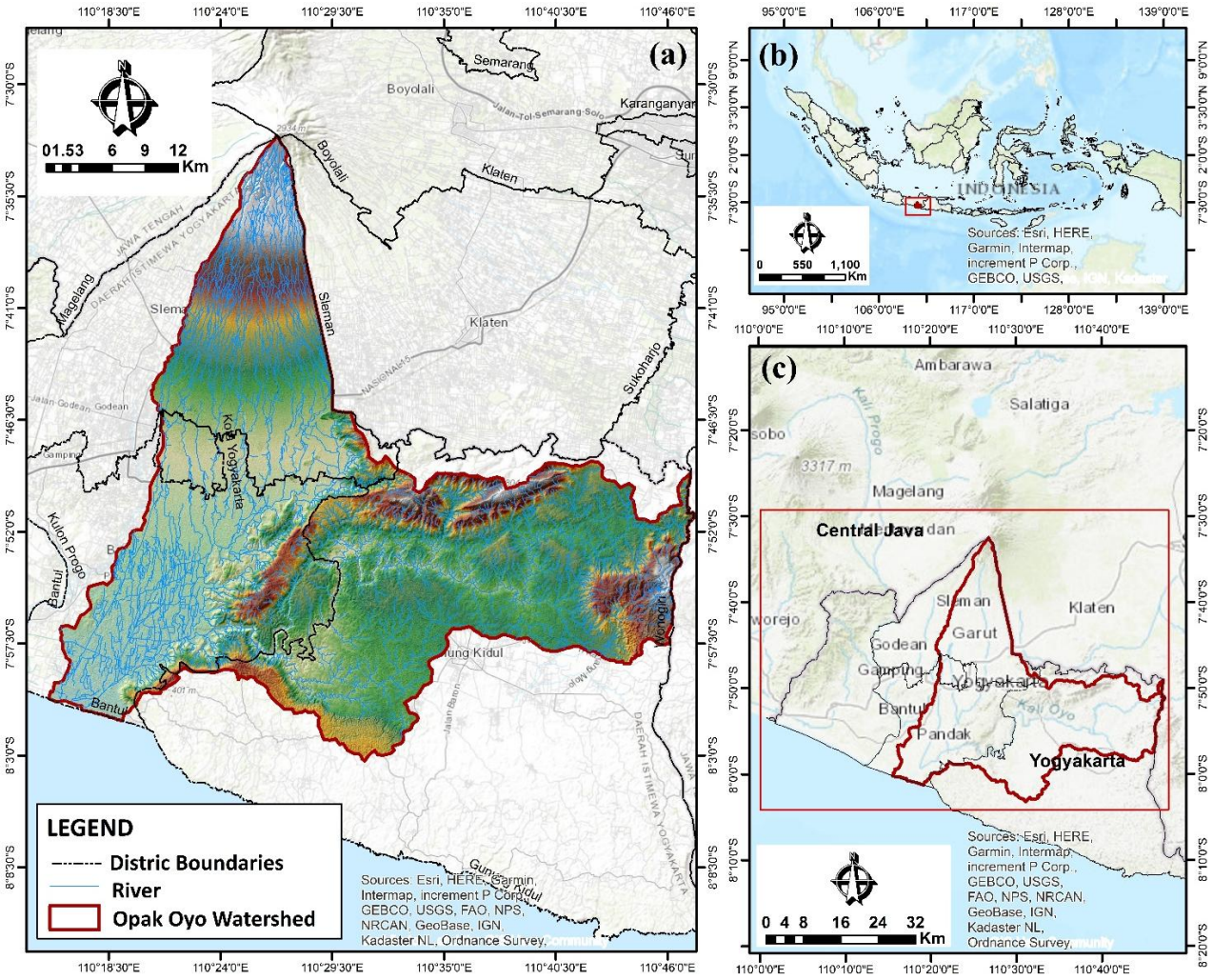

Figure 1. Study area. (a) Opak Oyo Watershed; (b) Region Scale; (c) Province Scale.

2.2. Data Collection

The research was conducted over three main stages: pre-field preparation, field verification, and post-field data processing. The pre-field stage focused on collecting and preparing secondary spatial datasets and analytical variables. The compiled variables included multi-temporal Landsat imagery (2004, 2014, 2024) for land-use and land-cover (LULC) analysis, DEMNAS-derived topographic parameters (elevation and slope gradient), lithology maps, river networks, road networks, administrative boundaries, population density, and official Volcano Hazard Zone (KRB) maps. Driving factors used in the Land Change Modeler (LCM) consisted of distance to rivers, roads, economic activity centers and government centers.

The field stage was conducted to validate the land-use classification results and tourism site locations through ground truth surveys using GPS coordinate recording and direct observation of land-cover categories (forest, agriculture, built-up areas, water bodies and open land). Tourism facilities were verified in terms of their spatial position, surrounding land use, and proximity to hazard zones. The post-field stage involved classification accuracy assessment using confusion matrix analysis, LCM-based land-use change simulation up to the year 2034, and spatial overlay analysis between tourism sites, topographic layers and KRB maps. The final outputs included thematic maps, statistical summaries and spatial interpretation to support sustainable tourism planning. The overall workflow distinguishing between pre-field, field and post-field activities is presented in Figure 2.

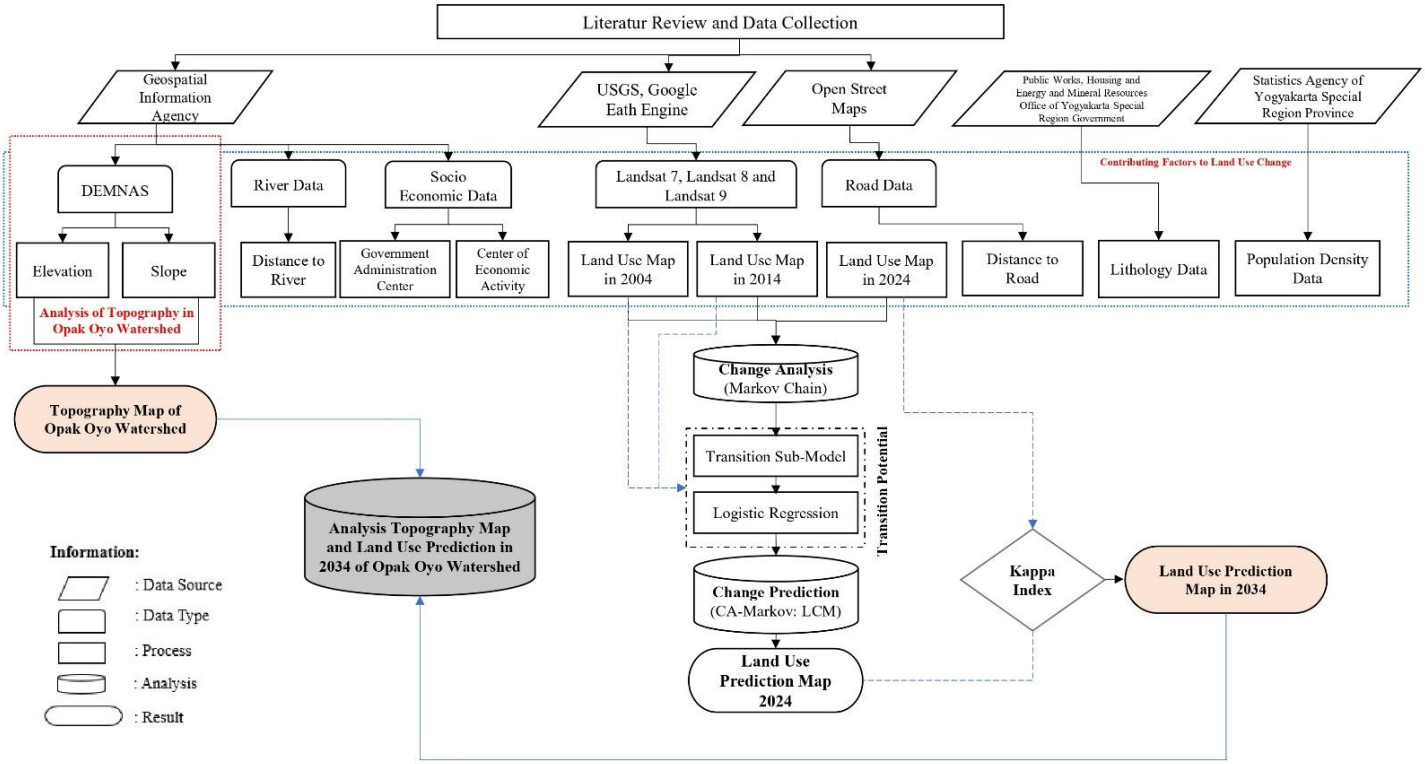

Figure 2. Research Framework.

Secondary data, such as road data, river data, lithology data and DEMNAS data, were used, obtained from several institutions. The secondary data were then processed utilizing remote sensing and GIS integration to create topographic maps and land-use change prediction maps in the OOW. The data employed can be seen in Table 1.

Table 1. Tools and Research Materials.

Type of Research Tool	Tools	Function
Hardware	Laptop	Data processing and operation of various software tools.
	Mobile Phone	Coordination of recording, digital notes and direct documentation capture in the field.
Software	Google Earth Engine	Data processing for land use analysis, computation and spatial data visualization.
	ArcGIS 10.5	Pre-processing of satellite imagery data and visualization of land use maps; processing of elevation, slope, lithology, and distance from rivers, roads, government centers, and economic activity centers, and population density data.
	Avenza Map 5.5	Documentation of data in the field using offline maps, such as marking waypoints and GPS tracks, measuring areas and adding photos or notes to locations.
	TerrSet 2020	Land use prediction data processing.
	Surfer 15	3D visualization of topographic data.
	CorelDRAW 2024	Visualization and design of all processed and generated maps.
Topography Data	DEMNAS Resolution 8.1m (https://tanahair.indonesia.go.id/)	Elevation interpretation and topographic analysis
Land Use Data for 2004, 2014 and 2024	• 2004: USGS Landsat 7 Collection 2 Tier 1 and real-time data calibrated top-of-atmosphere (TOA) reflectance • 2014: USGS Landsat 8 Collection 2 Tier 1 and real-time data calibrated top-of-atmosphere (TOA) reflectance • 2024: USGS Landsat 9 Collection 2 Tier 2 calibrated top-of-atmosphere (TOA) reflectance (https://earthexplorer.usgs.gov/)	Interpretation of land use data using the CART method

Table 1. Continued.

Type of Research Tool	Tools	Function
Slope Data	DEMNAS Resolution 8.1 m (https://tanahair.indonesia.go.id/)	Drivers of land use change in the Opak Oyo watershed, Yogyakarta Special Region, Indonesia
Lithology Data	Public Works, Housing and Energy and Mineral Resources Office of Yogyakarta Special Region Government (https://www.esdm.go.id/)	
Road Network Data	Open Street Map (OSM) (https://www.openstreetmap.org)	
River Data	Inageoportal, Indonesian Geospatial Agency (https://tanahair.indonesia.go.id/)	
Socio-economic Data (Administrative Center and Economic Activity)		
Population Data	Central Statistics Agency of Yogyakarta Special Region Province (https://jogjakota.bps.go.id/id)	

2.3. Data Analysis

2.3.1. Topographic Condition Analysis

Digital Elevation Model (DEM) data was utilized to understand the topographic conditions, visualizing the topography or land elevation based on deterministic interpolation results within the ecological boundary of the OOW. DEM data serve as one of the foundations in spatial analysis and modeling within the environment (Hasnaini *et al.,* 2024). In our case, the DEM data utilized was DEMNAS. With various types of data, DEMNAS had a spatial resolution of 0.27 arc-seconds using the Earth Gravitational Model (EGM) 2008 datum (Iswari & Anggraini, 2018). The integration of DEMNAS data could be transformed into topographic information related to elevation and slope. Digital Elevation Models have been widely used in several disaster studies; for example, for determining evacuation routes for volcanic disasters. The DEMNAS data were processed using spatial data processing software for slope and contour modeling. The slope and contour results were used in the creation of a topographic map containing information about elevation and slope in the OOW. The slope in the OOW was classified according to Van Zuidam (Zuidam, 1985), who divided it into several classes, as shown in Table 2.

Table 2. Slope Classification.

Class	Description
0 – 2%	Flat
3 – 15%	Moderate
16 - 25%	Moderate Steep
26 - 40%	Steep
>40%	Very Steep

Source: (Bermana, 2006; Harist et al., 2018).

2.3.2. Land Use Analysis and Prediction Modelling

Landsat 7, 8 and 9 satellite imagery was used to determine land use in the Opak Oyo Watershed. The data from the United States Geological Survey (USGS) were processed using the Google Earth Engine cloud computing platform (Ouchra *et al.,* 2023; Thi Anh Thu *et al.,* 2024). The use of Landsat imagery data in a time series using a combination of Landsat 7, 8,and 9 images was based on research by Kaur *et al.* (2023) to detect LULC in a time series from 2001/2002 to 2021, focusing on forest land cover in India. Landsat imagery was accessed from the GEE archive collection. Functions such as "ee.Filter.date ('start-date', 'end-date')" and "ee. filterMetadata" were used to filter the image collection depending on the date range. The images were then mosaicked once the availability of the images was screened.

Cloud cover was the necessary correction, processed for the least amount of cover (<10%), while cloud-free imagery was obtained by applying "CLOUD COVER," and "less˙than" values. Clouds and cloud shadows are handled using the cloudmasking function in GEE by utilizing the QA_PIXEL band of Landsat satellite imagery; the cloudmasking function is described in Figure 3a. For Landsat 7 satellite image data that experiences scan line errors, we used a script described in Figure 3b In this case, data with scan line errors were overlayed using imagery from the

previous or subsequent year that had no recorded errors. Subsequently, to classify Landsat, we first sharpened the satellite images using pan-sharpening (Figure 3c).

```
function CloudMasking(image){
    var cloudShadowBitMask = (1 << 3);
    var cloudsBitMask = (1 << 4);
    //var clearBitMask= (1 << 6);
    var qa = image.select('QA_PIXEL');
    var mask = qa
        .bitwiseAnd(cloudShadowBitMask).eq(0)
        .and(qa.bitwiseAnd(cloudsBitMask).eq(0));
    return image.updateMask(mask);
}
```

(a)

```
var img_fill = L7Mask.focal_mean(1.5, 'square', 'pixels', 10)
var CitraFilled= img_fill.blend(L7Mask)
var mosaic= CitraFilled.mosaic
```

(b)

```
"var sharpened2= ee.Image.cat[ hsv2.select('hue'), hsv2.select('saturation'),
L7Mask.select('B8').clip(AOI)
].hsvToRgb()"
```

(c)

Figure 3. Code Snippet of GEE Script. (a) Cloud Masking Script, (b) Line Error Correction Script, (c) Pan-sharpening Script.

Table 3. Opak Oyo Watershed Land Use Classification.

Classification	Description
Water Body (1)	Lake, River
Forest (2)	Forest, Vegetation
Built-up Land (3)	Built-up Land, Settlements and Road Networks
Agriculture (4)	Plantations, Fields and Rice Paddies
Vacant Land (5)	Mountains, Vacant Land and Sandstone Mines
Open Land (6)	Beach Sand
Cloud Cover (7)	Cloud, Atmospheric Distortion

For Landsat 8 and 9 data that did not experience scan line errors, the gap-filling process was not performed. However, the sharpening process was still performed to ensure that the data was used in image interpretation for land use data processing. Landsat data used to ensure temporal consistency for the long-term analysis (starting from 2000s), which covers the pre-eruption and post-eruption periods of Merapi. While Sentinel-2 offers higher resolution, its data record (starting in 2015) is insufficient for the long-term historical analysis required for this study. We ensured cross-calibration between Landsat sensors during the processing. Therefore, the study adopts a local land cover classification scheme based on the Indonesian National Standard, rather than the ESRI Land Cover (ESRI LC) dataset, due to the unavailability of ESRI LC data for the year 2004. Although the ESRI LC dataset provides a relatively high spatial resolution of 10 meters derived from Sentinel imagery, its temporal coverage does not extend to the earlier period required for this study, thereby limiting its suitability for long-term historical analysis. The land use classification is shown in Table 3.

Various types of data were used to assess the most influential factors in land-use changes in the OOW. They included geospatial data divided into two parameters: physical and socio-economic. The physical parameters included elevation, slope, lithology and distance from rivers, while the socio-economic ones included distance from roads, distance from government centers, distance from economic activity centers and population density data.

Land-use data processing was performed using the CART (Classification and Regression Tree) algorithm (Breiman), integrated within Google Earth Engine cloud computing. The script used was var classifier = ee.Classifier.smileCart().train({. The CART algorithm processing employed several bands available on Landsat satellite images, including band B1 (Blue), B2 (Green), B3 (Red), B4 (Near Infrared), B5 (Shortwave Infrared 1), and B7 (Shortwave Infrared 2). The CART

model is a machine learning algorithm widely used in land cover classification (Feizizadeh *et al.,* 2023; Pande *et al.,* 2024; Shang & Luo, 2021). The advantage of the CART algorithm for land use mapping is that it processes large datasets effectively, which is very important for regional scale mapping (Sun *et al.,* 2023), in addition, the algorithm also displays highly accurate performance in comparative analysis with other algorithms (Kadam *et al.,* 2025). Land-use map validation was performed using accuracy tests with a confusion matrix and Google Earth Engine cloud computing. The map results were compared with ground-checking results conducted in the field. Consequently, the maps processed with Google Earth Engine were considered valid and usable due to their accuracy of > 0.80, a value that was acceptable and interpreted as strong since it exceeded 0.80 (Ridwan *et al.,* 2017).

The land-use change model was used to analyze and predict land-use changes based on multi-temporal land-use maps. In our study, the MLP method with the Markov Chain algorithm was employed. This MLP-MC combination effectively captures the spatial and temporal dynamics of land use change. The method has been used to predict change over several decades, providing a comprehensive understanding of how land use patterns evolve over time (Ojelabi *et al.,* 2025). In our case, it determined the extent of land-use changes that occurred between 2004 and 2014 for predictions in 2024 and 2034, identifying land-use change conditions within the OOW, which formed the research boundary. The LCM (Land Change Modeler) land-use modeling results for 2024 were compared with the observed land-use results for 2024 using kappa index statistics (Yu *et al.,* 2023). The maps generated by the LCM model became predictive maps, which were then validated using several kappa parameters (K): kappa for grid cell location (Klocation), kappa for no information (Kno), kappa for strata-level location (KlocationStrata), and standard kappa (Kstandard) (Mishra *et al.,* 2018).

2.3.3. Tourism Risk Analysis

Tourism risk analysis was conducted to assess the level of exposure of tourism sites to volcanic hazards from Mount Merapi using a Geographic Information System (GIS)-based spatial approach. Tourism location data were obtained from official regional tourism agencies, field verification and digitization of high-resolution satellite imagery, and were subsequently georeferenced as point and polygon spatial layers. These tourism layers were overlaid with the official Mount Merapi Volcano Hazard Zone (KRB) map, which classifies the area into KRB I (low hazard), KRB II (moderate hazard) and KRB III (high hazard). This overlay process enabled the identification of the spatial distribution and concentration of tourism facilities within each hazard category, including areas potentially exposed to primary hazards such as pyroclastic flows and lava, as well as secondary hazards such as lahars.

To strengthen the assessment, the analysis also incorporated topographic parameters derived from DEMNAS, including elevation and slope gradients, as well as accessibility factors such as distance to roads and settlements. This approach allowed for the simultaneous evaluation of hazard exposure and spatial suitability for tourism development. The classified tourism risk results were then integrated with projected built-up land expansion generated by the LCM to identify potential future overlaps between tourism growth and hazard-prone zones. Through this integrated analysis, the study provides a spatially explicit basis for risk-informed tourism planning and sustainable development strategies in the Mount Merapi region.

3. Results and Discussion

3.1. Topography of the Opak Oyo Watershed

The Earth's physical surface conditions can be represented by topographic maps showing elevation and slope. Elevation refers to the height of a location above sea level, while slope refers to the percentage ratio between vertical distance (land height) and horizontal distance (flat land length) (Darmawan *et al.,* 2017; Triwahyuni, 2017). Slope shapes are generally influenced by erosion, land movement, and weathering processes. Information regarding the topography of the OOW was obtained by utilizing the National Digital Elevation Model (DEMNAS) with geospatial technology, as shown in Figure 4.

The topographic map of the OOW (Figure 4) shows significant variations in elevation and slope gradients. Based on the elevation map (Figure 4a), the area has an elevation range from 0 to over 300 meters above sea level. The southern part of the OOW is dominated by low-elevation areas (0–50 meters), while the northern part has higher elevations, reaching over 300 meters, which are likely to be hilly or mountainous regions. Areas with higher elevations generally have the potential to function as water catchment zones, whereas lowland areas are more vulnerable to surface runoff and flood risks. Table 4 shows the area coverage for the elevation in the Opak Oyo Watershed.

Meanwhile, the slope gradient (Figure 4b) indicates that the OOW has a diverse topography, ranging from flat plains to very steep hills. Table 5 shows the area coverage for slope gradients in the watershed.

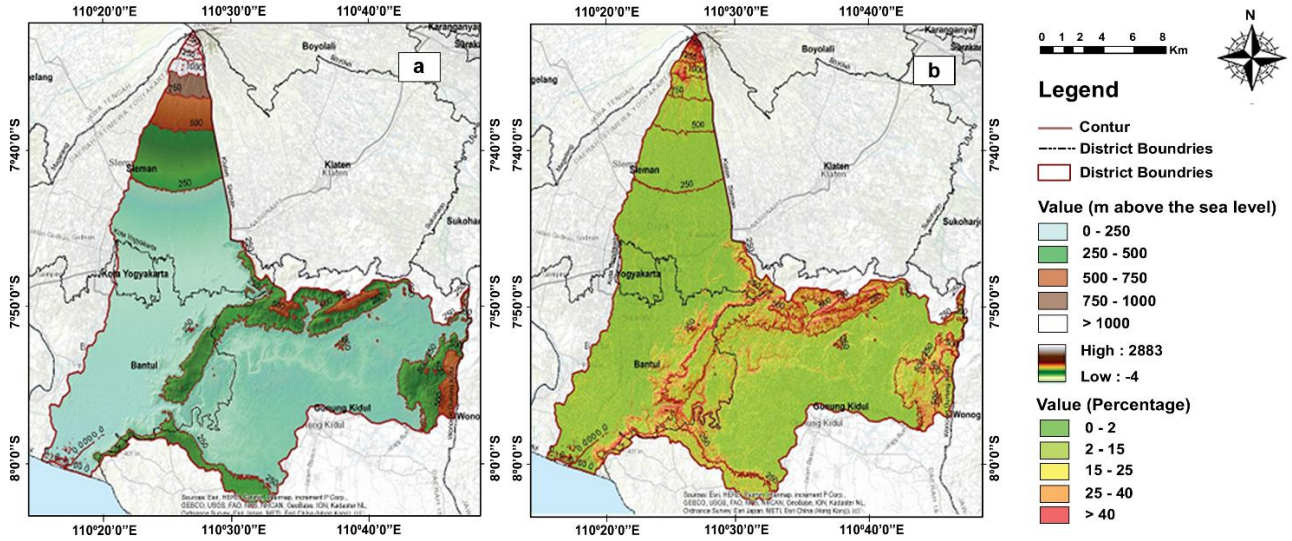

Figure 4. Topography Map of Opak Oyo Watershed, Indonesia. (a) Elevation, (b) Slope Gradient.

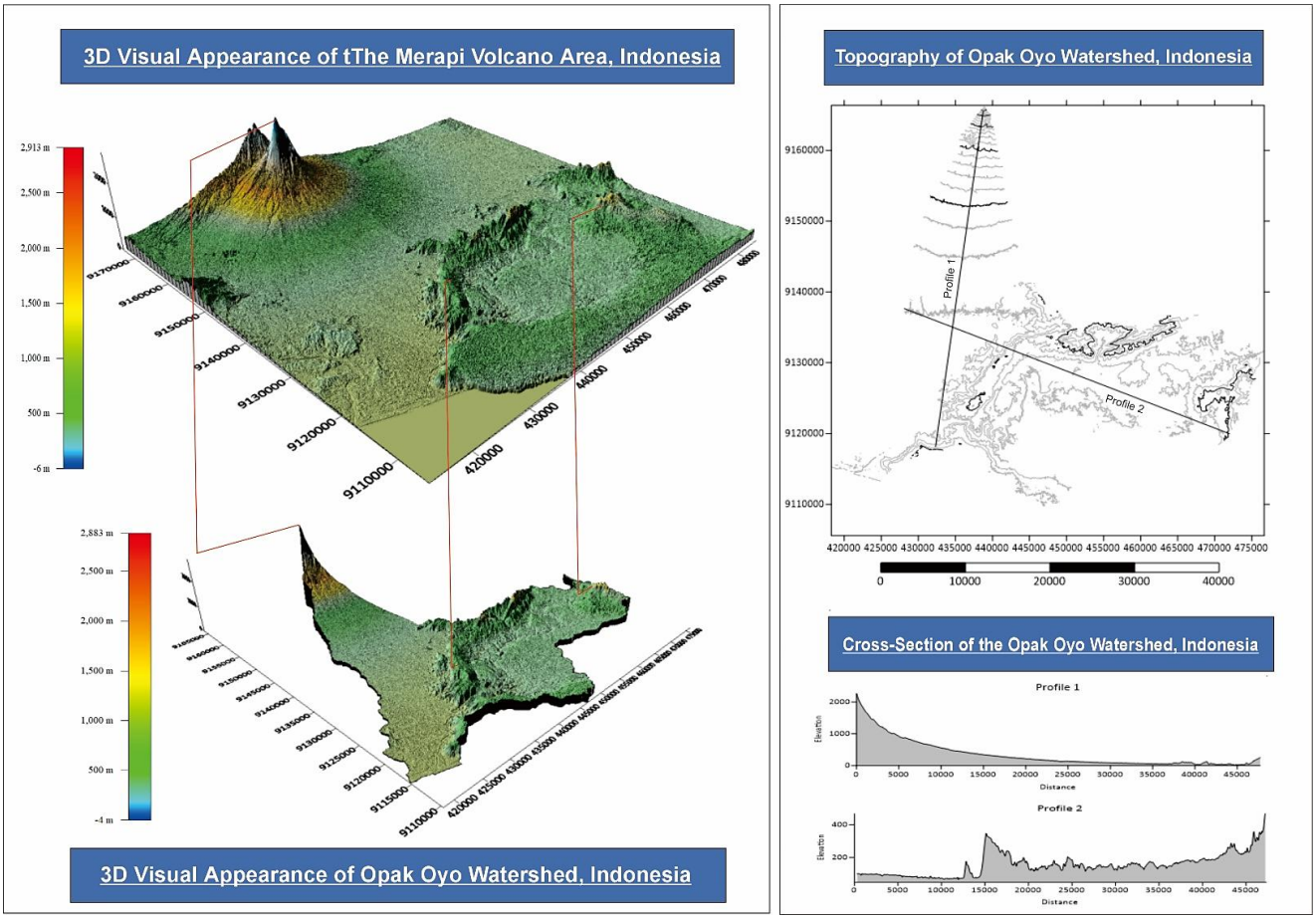

Figure 5. 3D Visualization of Mount Merapi and Opak Oyo Watershed, Indonesia.

Table 4. Elevation in the Opak Oyo Watershed

Elevation (meters above the sea level)	Area (km^2)	Percentage (%)
0 – 250	952.3	72.98
251 – 500	265.95	20.38
501 – 750	57.45	4.40
751 – 1000	13.99	1.07
> 1000	15.26	1.17
Total	1304.94	100

In the 3D visualization (Figure 5), it was observed that the central part of the OOW is bounded by hills with steep slopes. Furthermore, the region is dominated by lowland areas with gentle slopes, gradually descending towards the downstream areas, which directly border the sea.

Table 5. Slope Gradient in the Opak Oyo Watershed

Class	Description	Area (km^2)	Percentage (%)
0 – 2%	Flat	82.59	6.33
3 – 15%	Moderate	831.34	63.71
16 – 25%	Moderate Steep	204.5	15.67
26 – 40%	Steep	121.22	9.29
>40%	Very Steep	63.44	4.86
Total		1304.94	100

3.2. Land Use of the Opak Oyo Watershed in the Period 2004-2024 and Prediction Modeling

The CART algorithm is widely used to analyze land-use changes (Epie & Hull, 2025; Tekla *et al.,* 2024). Based on the data processing conducted using Google Earth Engine, it was found that the results were reliable and could be used for further processing, as shown in Table 6.

Table 6. Land Use Kappa Accuracy of the Opak Oyo Watershed using the CART Algorithm.

Years	Kappa Accuration
2004	0.962
2014	0.993
2024	0.990

A sampling method involving the stratified random sampling technique was used to determine the location points of the previously processed 2024 land use map results. This was done to validate the results of the satellite image classification processing. This method was employed so that the sample distribution was evenly distributed across all land use classes (all classes were represented). The maps processed using the CART algorithm with the training data used consisted of 582 points for total landuse, which were then validated using Google Earth imagery with 182 validation points, resulting in a user accuracy of 0.945, a kappa accuracy of 0.928, and an overall accuracy value of 0.945 (or 94.5%).This indicated that the map was accurate and could be considered valid for further use, as its accuracy was >0.80. Based on the results of the data processing, a temporal analysis was then conducted on the land-use changes in the OOW area. It was found that from 2004 to 2024 significant changes had taken place (Table 7).

Table 7. Area of Land Use Changes in the Opak Oyo Watershed in 2004, 2014 and 2024.

Land Use	Area (km^2)			Difference in Area (km^2)			Percentage of Area (%)		
	2004	2014	2024	2004 - 2014	2014 - 2024	2004 - 2024	2004	2014	2024
Waterbody	17.71	24.33	24.38	6.62	0.05	6.67	1.36	1.86	1.87
Forest	466.62	560.95	433.19	94.33	-127.76	-33.43	35.76	42.99	33.20
Built-up Land	191.88	134.97	182.09	-56.91	47.12	-9.79	14.71	10.34	13.95
Agriculture	425.84	458.93	518.36	33.09	59.43	92.52	32.63	35.17	39.72
Vacant Land	15.63	7.79	13.96	-7.84	6.17	-1.67	1.20	0.60	1.07
Open Land	1.16	6.54	6.19	5.38	-0.35	5.03	0.09	0.50	0.47
Cloud Cover	186.02	111.36	126.71	-74.66	15.35	-59.31	14.26	8.53	9.71
Total	1304.94	1304.94	1304.94				100.00	100.00	100.00

Based on Table 7, during the period from 2014 to 2024 there was a significant increase in built-up areas, with the addition of 47.12 km². This was part of the local government's efforts in rehabilitation, reconstruction and recovery in the housing, infrastructure, social and productive economic sectors as a result of the eruption of Mount Merapi and the earthquakes in the region. Furthermore, land use in the OOW was shown to be generally characterized by land conversion from dryland agriculture, shrubs, forests and open land into built-up areas. This change in land-use patterns led to a reduction in water absorption capacity, increasing surface runoff (Nugroho *et al.,* 2018). A visualization of land-use changes in the OOW from 2004 to 2024 can be seen in Figure 6.

Water, agricultural and open land types also saw increases in area. The expansion of water areas from 2004 to 2024 was part of an integrated watershed management effort, particularly for the OOW, as stipulated by the Governor's Decree of the Special Region of Yogyakarta No. 285/KEP/2014. The increase in agricultural areas during the period 2004-2024 in the region influenced the hydrological response of the Opak Watershed. Agricultural land dominated the Opak Watershed, covering 518.36 km² in 2024. Generally, the increase in agricultural land use,

particularly for mixed dryland agriculture, was balanced by the expansion of settlement areas. Agricultural land in the OOW was utilized for the cultivation of food crops such as corn, upland rice, soybeans and cassava. According to a study simulating existing land use dominated by agriculture and settlements (Widiatmoko *et al.,* 2020), the KAT (Annual Runoff Coefficient) value was high at 0.4, with a River Regime Coefficient of 85.16, also in the high category. This suggests that a significant amount of rainfall became direct runoff. These findings indicate that land-use changes impacted the hydrological response of the watershed. Therefore, a watershed management planning strategy is needed to optimize the hydrological function of the area. Additionally, an increase in open land area of approximately 5.03 km² occurred between 2004 and 2024.

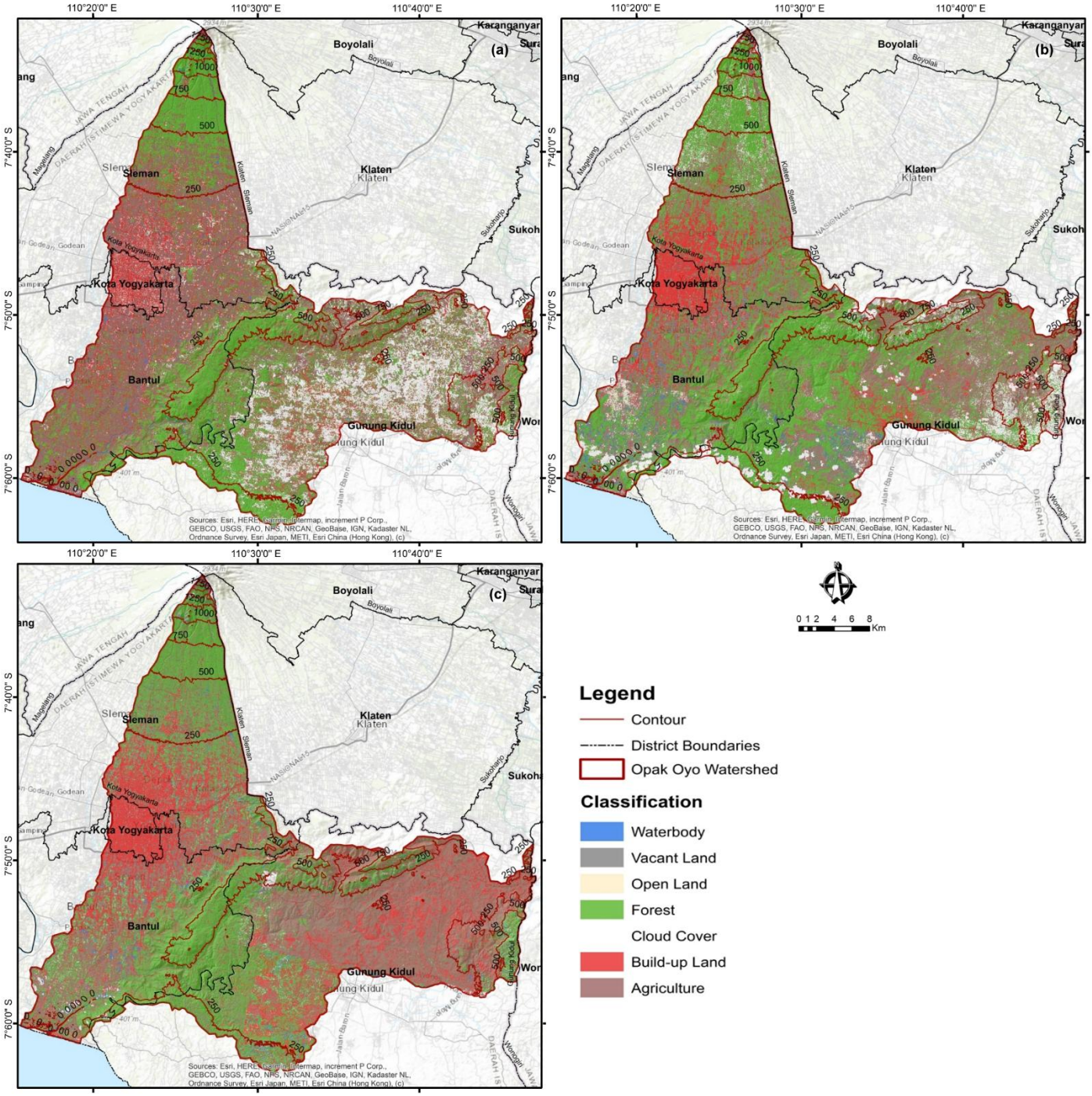

Figure 6. Visualization of Land Use Changes in the Opak Oyo Watershed. (a) 2004, (b) 2014, (c) 2024.

Land use in the OOW in 2004 and 2014 was employed to develop a Land Change Modeler (LCM) model, with a scenario of increased built-up land in 2024, using the MLP Neural Network-Markov Chain algorithm. In our study, the algorithm was used with the following criteria: a) a final learning rate of 0.0001; b) a momentum factor of 0.5; c) a sigmoid constant of 1.0; and d) eight input layer neurons, four hidden layer neurons and two output layers. These criteria were based on RMS of 0.01, 10000 iterations, and an accuracy rate of 100%. An input layer of eight neurons was used

to represent the number of driving variables used in the model, while the hidden layer was employed to process complex non-linear relationships.

The low learning rate value of 0.0001 indicates that the model learns very carefully and slowly, which is good for achieving high accuracy without overshooting the optimal solution, although it requires longer computation time. A momentum factor value of 0.5 is balanced between maintaining the previous learning direction and adjusting to new data. An iteration value of 10,000 indicates the maximum number of learning cycles (epochs), while an RMS error value of 0.01 is the average error tolerance limit. If the average prediction error falls below 0.01, the model is considered sufficiently accurate and stops learning. The LCM simulation with a built-up land increase scenario of OOW in 2024 was built on a standard but rigorous algorithmic foundation. The validity of the prediction results (Table 8) depends heavily on how well the eight input variables (neurons) represent the reality of land change drivers in the field, as the machine parameters themselves are set for high mathematical accuracy. These criteria represent the default settings of the LCM model. The results are shown in Table 8.

The results of the calibration and validation of the LCM model using the multi-layer perceptron (MLP) algorithm show varying but robust levels of reliability across all land transition variables. These findings are in line with recent studies that consider MLP to be one of the most effective algorithms for handling the non-linear dynamics of land cover change compared to conventional methods (Subiyanto *et al.,* 2019). As detailed in Table 8, the model shows high stability in the learning process, characterized by consistently low training RMS and testing RMS values, with a very small difference between them. For example, in the transition from vacant land to built-up land, the training RMS was recorded at 0.3751 and the testing RMS at 0.3744. The closeness of these values confirms that the model experienced no overfitting and was able to generalize well on the test data.

The close RMS values in the query indicate that the model was effectively validated and could generalize well to new data, a crucial indicator of validity in neural network-based spatial modeling (Sabiri *et al.,* 2022). Overall, the highest accuracy rate was achieved in predicting the change from open to built-up land, at 90.44%, with a very dominant transition skill (0.8901). This shows that the MLP algorithm is very effective in capturing spatial patterns in open land. Although the accuracy for the transition to agriculture is slightly lower (67.25%), the model still maintains acceptable predictive capabilities given the complexity and heterogeneity of agricultural patterns, which often pose challenges in tropical region modeling (Sajan *et al.,* 2022). Based on the above MLP results, it was found that the ROC (receiver operating characteristic) value ranged from 67.25% to 90.44%, falling between 50% and 100% (Table 8), indicating that the model used, along with the eight variables, was significant and influenced land-use changes. As demonstrated in Table 8, it was found that each model had dominant and non-dominant factors affecting land-use changes in the Opak Oyo Watershed.

Table 8. LCM Model Results with the MLP Neural Network Algorithm for a Built-up Land Expansion Scenario in the Opak Oyo Watershed.

Bound Variable Land Use Change	Training RMS	Testing RMS	Accuration Rate of Model	Model Skill Breakdown by Transition & Persistence		Most Influential Factors in Land Use Change	Least Influential Factor in Land Use Change
				Transition	Persistence		
Water to Built-up Land	0.3607	0.3634	81.88%	0.6327	0.6425	Distance from River	Population Density
Forest to Built-up Land	0.4399	0.4419	70.45%	0.4397	0.3777	Distance from Road	Distance from River
Agriculture to Built-up Land	0.4598	0.4615	67.25%	0.4916	0.1981	Distance from Road	Lithology
Vacant Land to Built-up Land	0.3751	0.3744	80.10%	0.8840	0.3275	Distance from Center of Economic Activity	Population Density
Open Land to Built-up Land	0.2741	0.2775	90.44%	0.8901	0.5979	Lithology	Slope
Cloud Cover to Built-up Land	0.3719	0.3750	78.83%	0.4083	0.7429	Population Density	Distance to River

The land-use modeling results using the Land Change Modeler MLP-Markov Chain model with a built-up land expansion scenario for 2024 (Figure 7b), were compared with the actual land-use map for 2024 in the OOW (Figure 7a). Kappa statistics for quantity and location were obtained based on an evaluation of the predicted compared to the observed land use. The statistics show that the Kno value was 0.8176, the Klocation value was 0.8053, the KlocationStrata value was 0.8053, and the Kstandard value was 0.7206. All kappa index values obtained between 0.72 and

0.80 indicate significant agreement, with values between 0.81 and 0.99 indicating near-perfect agreement (Azizah *et al.,* 2023).

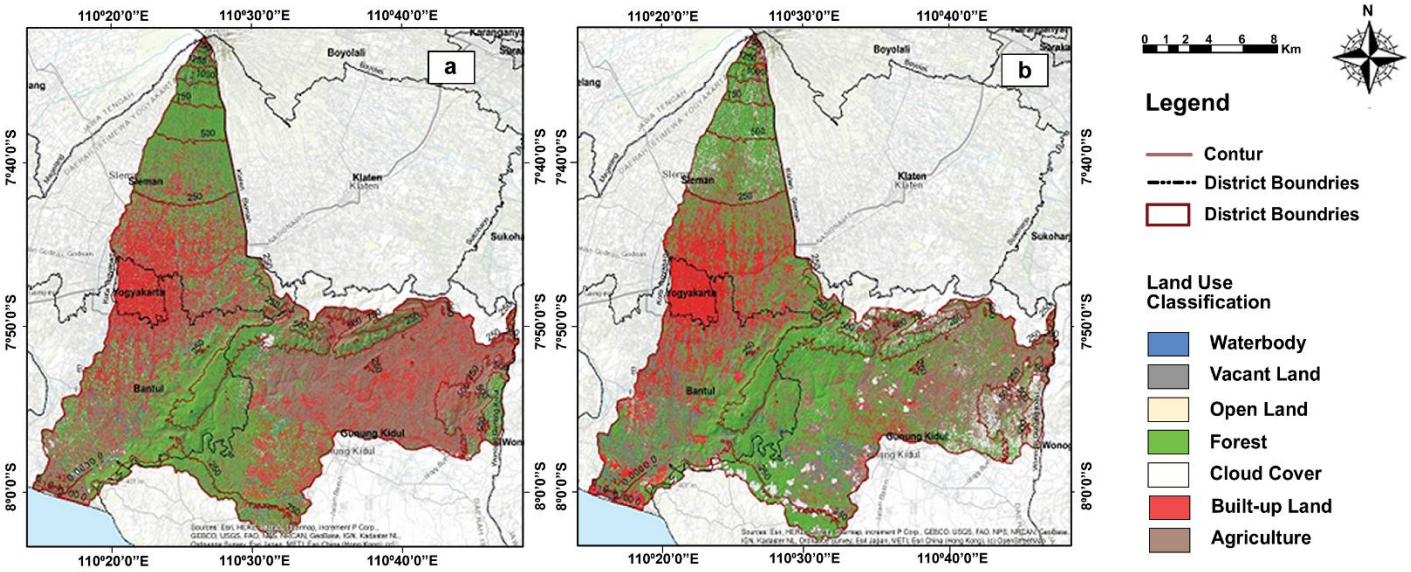

Figure 7. Land Use Map of the Opak Oyo Watershed. (a) Real Data in 2024; (b) Predicted Land Use Change Based on the LCM Model with a Built-up Land Expansion Scenario for 2024.

Furthermore, the validated model for 2024 was used to model land use with a built-up land expansion scenario for 2034. From the predicted land use map for 2034 (Figure 8), it was found that in that year (Table 9), the area of water bodies in the OOW will cover 22.86 km², forest areas will cover 523.94 km², built-up land will cover 213.87 km², agricultural areas will cover 422.12 km², barren land will cover 5.55 km², open land will cover 4.92 km², and cloud cover will account for 100.15 km². Compared to the 2024 land-use results, several land-use category experienced significant changes and area expansions. Reductions occurred in water bodies, agricultural areas, barren land, open land and cloud cover. In contrast, other categories, such as forests and built-up land, experienced area expansions, at 6.95% for forests and 3.53% for built-up land, between 2024 and 2034. However, water bodies decreased by 0.12%, agricultural areas by 7.67%, barren land by 0.56%, open land by 0.10%, and cloud cover by 2.04% between 2024 and 2034.

Table 9. Opak Oyo Watershed Area in 2014, 2024 and 2034.

Land Use	Area (km²)			Difference Area 2024-2034	
	2014	2024	2034	Difference Area (km²)	Difference Area (%)
Waterbody	17.71	24.38	22.86	-1.52	-0.12
Forest	466.62	433.19	523.94	90.75	6.95
Built-up Land	191.88	182.09	228.13	46.04	3.53
Agriculture	425.84	518.36	418.22	-100.14	-7.67
Vacant Land	15.63	13.96	6.68	-7.28	-0.56
Open Land	1.16	6.19	4.92	-1.27	-0.10
Cloud Cover	186.02	126.71	100.15	-26.56	-2.04
Total	1304.94	1304.94	1304.94		

b.

Temporal analysis of the changes in land cover revealed two contrasting transition patterns between the historical observation period (2014–2024) and the prediction scenario (2024–2034). During the decade from 2014 to 2024, the landscape of the region was dominated by significant deforestation, with forest cover shrinking dramatically by 127.76 km² (-22.7%). This decline correlates positively with the expansion of agricultural areas, which increased by 59.43 km², and of built-up land, which increased by 47.12 km². This indicates strong anthropogenic pressure, with the conversion of forest land to cultivation and settlement areas being the main drivers of landscape change.

However, the 2034 land use scenario projects a reversal of ecological trends. The agricultural sector is predicted to experience a massive contraction, with a reduction in area of 100.14 km². This decline appears to be offset by land rehabilitation programs or natural succession, marked by the restoration of 90.75 km² of forest areas. Several forest and land rehabilitation initiatives are being undertaken, such as implementation of the *Indonesia's FOLU Net Sink 2030* program

by the Ministry of Environment and Forestry, and the *Tree Collective Gunungkidul 2025* program, which involves the planting of 15,000 multi-purpose tree species (MPTS). This program is organized by the Javlec Indonesia Foundation, JejakIn, and the Wana Makmur and Wana Lestri Community Forest Farmer Groups (Dharmawan & Pratiwi, 2023), and involves the conversion of abandoned or critically degraded Sultan Ground (SG) and Pakualaman Ground (PAG) around the OOW into conservation forests or green open spaces.

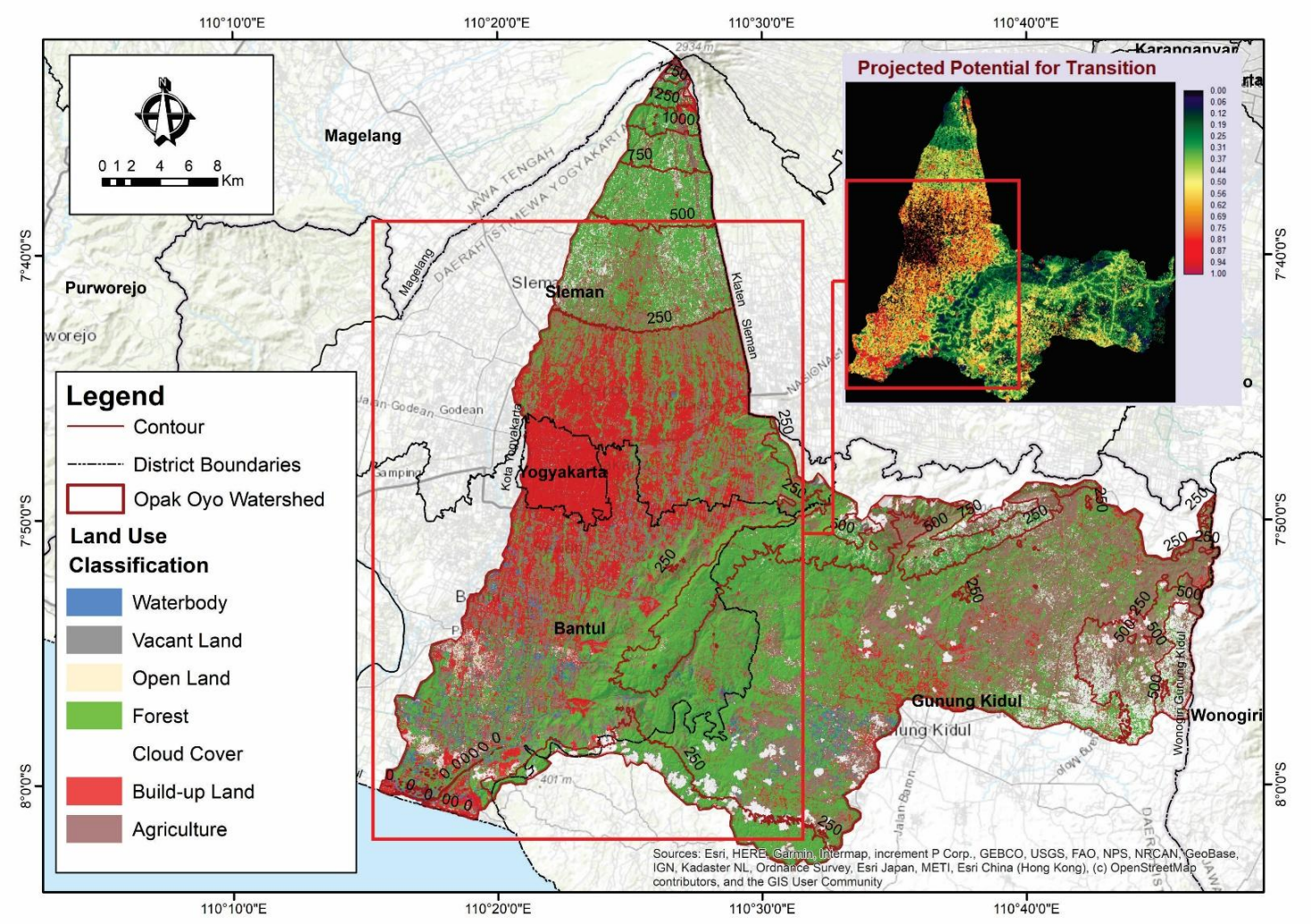

Figure 8. Map of Predicted Land Use Change using the LCM Model with the MLP-Markov Chain Algorithm referring to a Built-up Land Expansion Scenario for 2034.

Despite fluctuations growth in the forestry and agriculture sectors, urbanization shows a consistent linear growth trend. Built-up land is projected to continue increasing by 46.04 km² during the 2024–2034 period, absorbing vacant land and some agricultural land, bringing the total built-up area to a peak of 228.13 km². This phenomenon confirms that even though ecological restoration efforts are projected to occur, physical urban expansion remains a permanent variable in the spatial dynamics of the region.

In Figure 8, it can be seen that the conversion of land into built-up areas has primarily spread from the central part of the OOW toward the coastal areas. This is shown by the projected potential for transition, where the red visualization with a value of 1 indicates the potential for land conversion into built-up areas in the OOW (Figure 8). As shown in Table 8, the most dominant factor influencing the conversion of water bodies into built-up land is the distance from rivers; the conversion of forests and agricultural areas into built-up land is influenced by the distance from roads; the conversion of barren land into built-up land is influenced by the distance from economic activity centers; and the conversion of open land into built-up land is influenced by lithology.

3.3. Integration of Topographic Data and the LCM Model with Tourism Activities in the Opak Oyo Watershed

Factors related to topography and slope gradients have influenced the potential for and development of tourism in the OOW. Tourist attractions have differing morphological conditions and

accessibilities. Different landforms have varying hazard potentials due to their distance from the eruption center and slope gradients (Ashari, 2018). The tourism areas in OOW are evenly distributed in the upper, middle and lower parts of the watershed (Figure 9 and Table 10).

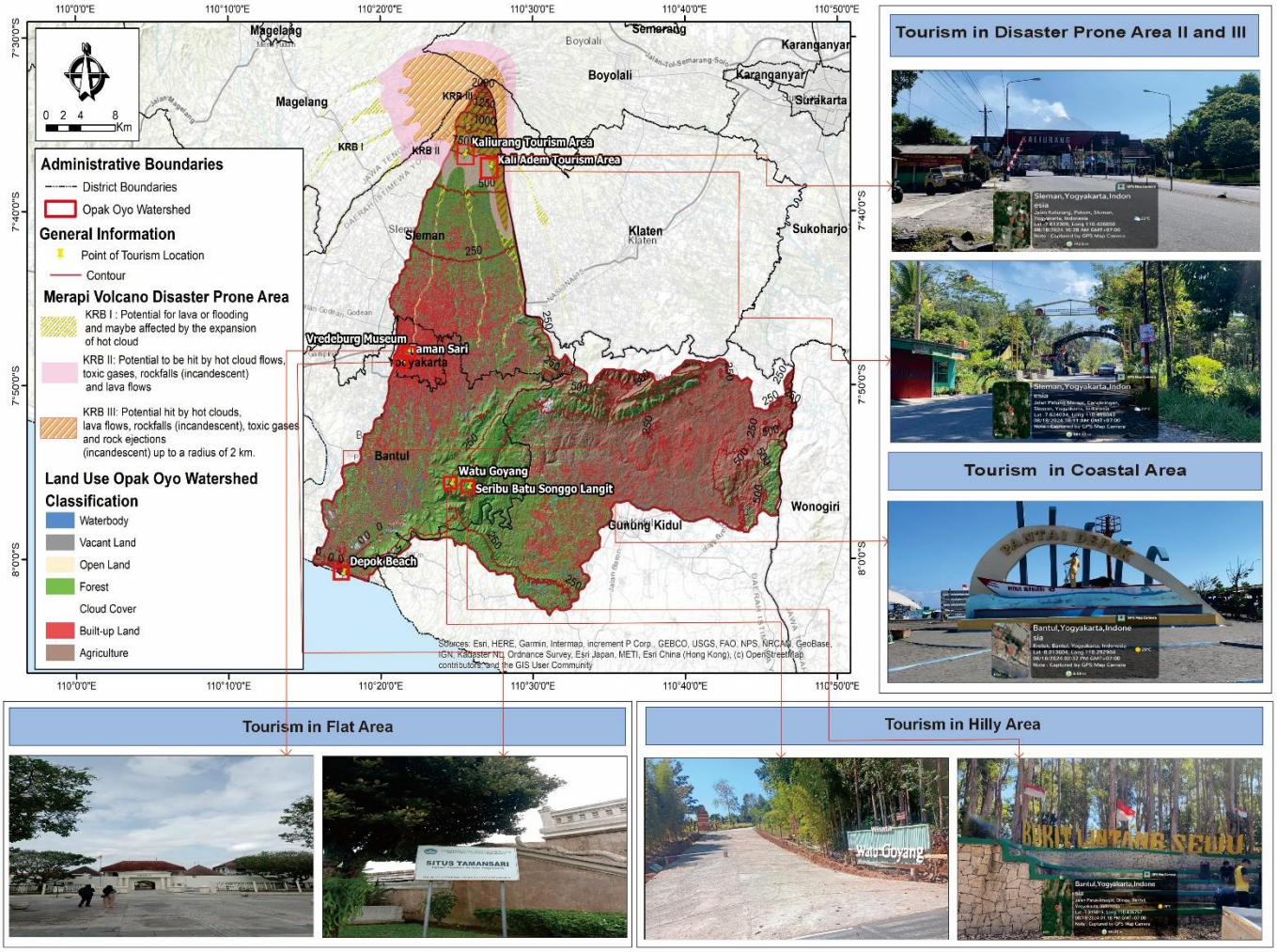

Figure 9. Tourism Area Map of OOW, Special Region of Yogyakarta, Indonesia, 2024.

Table 10. Tourism Site in Volcanic Disaster Prone Area.

Volcanic Hazard Zone (Disaster-Prone Area)	Description	Tourism Site
Disaster-Prone Area (KRB) I - Low Risk	Merapi volcano disaster-prone area subject to lava flows or flooding and may be affected by the spread of hot clouds.	Ledok Sambi Lor Sambi
Disaster-Prone Area (KRB) II – Medium Risk	Merapi volcano disaster-prone area potentially affected by hot clouds, toxic gases, falling rocks (incandescent) and lava flows.	Heha Forest Merapi Golf Club Lava Tour Merapi Suraloka Interactive Zoo Luma Roots Lightscape Ullen Sentalu Museum
Disaster-Prone Area (KRB) III – High Risk	Merapi volcano disaster-prone area often affected by hot clouds, lava flows, rockfalls (incandescent), toxic gases, and rock ejections (incandescent) within a radius of 2 km.	The Lost World Castle Alien Stone Merapi Mini Sisa Hartaku Museum ATV Kaliurang Tour Kalikuning Park Kali Kuning Park Cliff Tourism Gendol Cliff, Mount Merapi Kaliadem Bunker Tour Mbah Maridjan Memorial Museum Klangon Hill

It was found that the tourism areas were located at elevations ranging from 2883 meters to 250 meters above sea level, with steep slopes in the upper region, which is part of the volcanic hazard-prone areas of Mount Merapi. The tourism in this region is known as disaster tourism. Based on the disaster prone map (Figure 10), the distribution of tourism areas was concentrated in the

volcano hazard-prone areas, mainly clustering in KRB III (Table 11) This area should have been vulnerable for use as a residential and activity zone because it has a high potential for pyroclastic flows, lava flows, volcanic bombs, toxic gases and new collapses. However, due to various beliefs, people have long settled on the slopes of Mount Merapi, and the population in this area continues to grow (Widodo *et al.,* 2024). In the Regent's Regulation No. 20 of 2011 on the Merapi Volcanic Hazard Zone, KRB III is indeed stated to be unsuitable for residential or tourism development because it could endanger people or visitors during disasters. Unfortunately, some people are still exploiting KRB III as a profitable tourist attraction, while people choose to live in the zone to be close to the source of their livelihoods. Several tourist attractions in KRB III are still facing issues related to permits from the Sleman Regency Government. While tourism near Mount Merapi had boosted the economy, the safety of visitors and the local community needs to be prioritized.

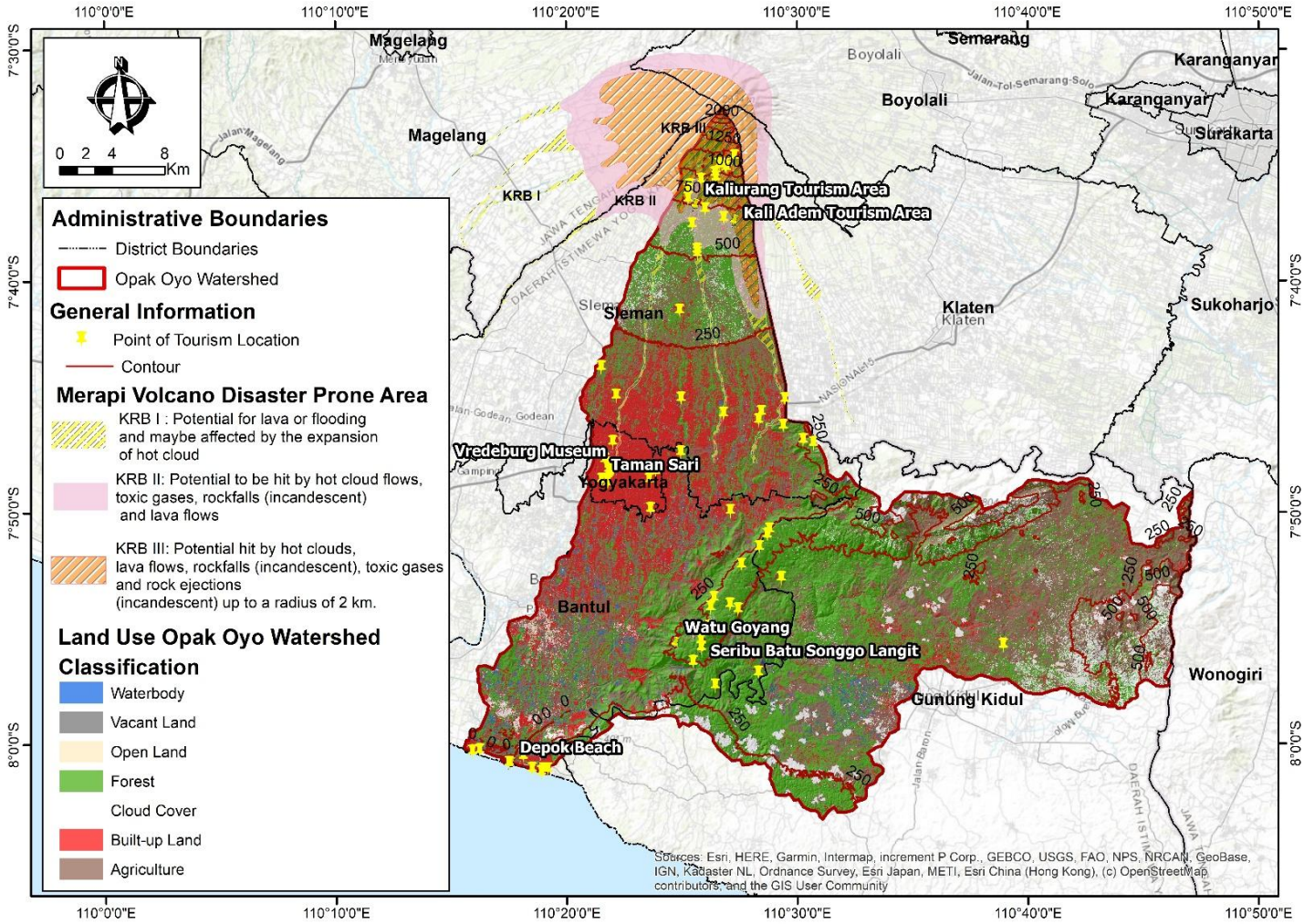

Figure 10. Tourism Areas in Relation to the 2034 Land Use Map Model Using the MLP-Chain Markov Algorithm.

As shown in Figure 10, the change in land-use to built-up areas within the disaster-prone area (KRB) of Mount Merapi in 2034 appears to be very extensive. If this trend continues and encroaches further into the disaster-prone radius, the consequences will be catastrophic, potentially resulting in significant casualties. Therefore, a disaster mitigation-based policy approach is necessary and should be implemented by various relevant stakeholders. One of the key measures is disaster preparedness training and readiness programs for local communities, particularly for tourism operators located in disaster-prone areas. The Regional Disaster Management Agency (BPBD) should intensify such efforts, as they play a critical role in ensuring public safety. Training and evacuation drills for tourism operators who act as first responders during evacuations must be regularly held to ensure that evacuation procedures are conducted in a systematic and effective manner in the event of a disaster.

Additionally, the Regional Development Planning Agency of Sleman Regency should play an active role in disaster mitigation-based spatial planning. This includes restricting development in

high-risk zones (red zones), designing emergency evacuation routes, and relocating vital infrastructure to minimize the direct impact of a potential Mount Merapi eruption, particularly in response to the projected increase in built-up areas within tourism zones by 2034. The government could also implement a disaster-mitigation-based tourism concept, whereby visitors not only experience the natural beauty of the area, but also receive education on potential disasters and appropriate response measures. Tourism development should not only prioritize economic aspects, but also ensure safety and environmental sustainability. Such sustainability should be supported by strict regulations regarding land use and tourism facility development to ensure alignment with disaster mitigation strategies. The findings of this study are in line with the research conducted by (Muthohar *et al.,* 2020), who found that some tourist attractions in Mount Merapi volcano KRB III lack disaster evacuation signs.

Table 11. Tourism Sites in Volcanic Disaster-Prone Areas in 2004, 2014, 2024 and 2034.

Disaster Prone Area	Tourist Site	Category of Land Use			
		2004	2014	2024	2034
Disaster Prone Area (KRB) I - Low Risk	Ledok Sambi	Forest	Forest	Forest	Forest
	Lor Sambi	Forest	Forest	Forest	Forest
Disaster Prone Area (KRB) II – Medium Risk	Heha Forest	Forest	Forest	Forest	Forest
	Merapi Golf Club	Forest	Forest	Forest	Forest
	Lava Tour Merapi	Forest	Agriculture	Vacant Land	Agriculture
	Suraloka Interactive Zoo	Forest	Forest	Build-Up Land	Built-Up Land
	Luma Roots Lightscape	Forest	Forest	Forest	Forest
	Ullen Sentalu Museum	Forest	Forest	Forest	Forest
Disaster Prone Area (KRB) III – High Risk	The Lost World Castle	Forest	Agriculture	Built-Up Land	Agriculture
	Alien Stone Merapi	Forest	Agriculture	Forest	Agriculture
	Mini Sisa Hartaku Museum	Forest	Forest	Agriculture	Forest
	ATV Kaliurang Tour	Forest	Agriculture	Forest	Agriculture
	Kalikuning Park	Forest	Forest	Forest	Forest
	Kali Kuning Park Cliff Tourism	Water-body	Vacant Land	Vacant Land	Vacant Land
	Gendol Cliff, Mount Merapi	Forest	Agriculture	Agriculture	Agriculture
	Kaliadem Bunker Tour	Agricul-ture	Built-Up Land	Open Land	Vacant Land
	Mbah Maridjan Memorial Mu-seum	Forest	Agriculture	Agriculture	Agriculture
	Klangon Hill	Forest	Foest	Forest	Forest

However, efforts towards disaster mitigation in terms of accessibility to tourism areas have been initiated, but are hindered by signs and potholes in the roads. Moreover, there is still no well-designed disaster management in the tourism areas. Therefore, there is a need for both structural and non-structural disaster mitigation initiatives in the area, tailored to the morphological characteristics and hazard potentials in order to preserve the terrestrial ecosystem through sustainable land and tourism management, in line with goals 11 and 15 of the Sustainable Development Goals. Consequently, the research findings could serve as a basis for local governments and tourism area managers to formulate land-use policy guidelines integrated with effective regional spatial planning, prioritizing economic growth that synergizes with the considerations of volcanic hazard-prone areas. The study has several limitations that should be considered when interpreting the results. First, it utilizes several Landsat sensors, namely Landsat 7, 8 and 9, each of which has different spectral bandwidths for land use interpretation using natural color composite imagery (red, green and blue).

Therefore, additional processing related to data normalization for each image scene is required when conducting more in-depth analyses involving the spectral values of the imagery, such as the calculation of vegetation density indices (e.g., NDVI). Second, although DEMNAS provides relatively high-resolution national elevation data, micro-topographic variations and rapid post-eruption morphological changes may not be fully captured, particularly in areas affected by newly deposited volcanic materials or intensive erosion processes. Third, the tourism risk analysis in the study focuses primarily on spatial exposure within KRB, but does not quantitatively measure vulnerability components such as the structural resilience of buildings, evacuation preparedness, visitor density, or the adaptive capacity of local communities. In addition, social, cultural and economic factors influencing tourism development decisions are represented only indirectly through spatial variables. Future research could incorporate more dynamic hazard simulations, multi-criteria risk indices, and participatory approaches to enrich sustainable tourism planning analysis in volcanic hazard-prone regions.

4. Conclusion

The findings of the study confirm that topographic characteristics, particularly elevation and slope gradients in the OOW, play a fundamental role in shaping spatial development and tourism expansion patterns. The integration of DEM-based topographic analysis with the Land Change Modeler (MLP–Markov Chain) enabled a detailed simulation of land-use dynamics from 2004 to 2034, reflecting both historical trends and projected changes. The 2034 simulation indicates an increase in forest and built-up areas, accompanied by a decline in water bodies, agricultural land, barren land and open land. This projected expansion of built-up areas highlights the continuing pressure of tourism and settlement growth, especially in zones with favorable accessibility and morphological conditions.

A critical insight emerging from the projection is the spatial overlap between future built-up expansion and the Mount Merapi volcano hazard zone. The growth of tourism facilities and supporting infrastructure within hazard-prone areas increases exposure to volcanic threats such as pyroclastic flows, ashfall and lahar events. If land conversion continues without the integration of topographic constraints and hazard zoning considerations, the region may face heightened vulnerability, including potential casualties and infrastructure damage. The findings emphasize that tourism development in volcanic landscapes must be guided by risk-informed spatial planning rather than purely economic considerations.

From a practical perspective, the results provide strategic input for regional planning institutions such as BAPPEDA Sleman Regency, BPBD, and other policymakers. Spatial planning policies should integrate high-resolution topographic analysis, predictive land-use modeling, and hazard zonation to guide tourism development toward safer and environmentally suitable areas. Strengthening zoning regulations, enforcing environmentally sensitive land conversion controls, and embedding disaster risk reduction principles into tourism master plans are essential steps toward achieving sustainable development in the Merapi region.

Acknowledgements

The authors are grateful to State University of Malang (UM) for supporting this research activity through the RKI (Riset Kolaborasi Indonesia) grant, as well as Gadjah Mada University, Padjajaran University, and Université Paris 1 Panthéon-Sorbonne for their support during field research and during the paper preparation process. The autors are grateful to all the agencies that have helped in the research. The autors also grateful to the local government at the district level in Yogyakarta, who helped in the research**.**

Author Contributions

Conceptualization: Bachri, S., Wibowo, S. B., Sunardi, S., Lavigne, F.; **methodology**: Prastiwi, M. R. H.; **investigation**: Hakiki A. R., Hidiyah, T. M., Putri, N. R. C.; **writing—original draft preparation**: Bachri, S.; **writing—review and editing**: Bachri, S.; **visualization**: Prastiwi, M. R. H. All authors have read and agreed to the published version of the manuscript.

Conflict of interest

All authors declare that they have no conflicts of interest.

Data availability

All data generated or analysed during this study are included in this published article.

Funding

This research received no external funding

References

Alfama, V., Henriques, M. H., & Barros, A. (2024). The challenging nature of volcanic heritage: the Fogo island (Cabo Verde, W Africa). *Geoheritage*, 16(2), 34.

Andreastuti, S. D., Paripurno, E. T., Subandriyo, S., Syahbana, D. K., & Prayoga, A. S. (2023). Volcano disaster risk management during crisis: implementation of risk communication in Indonesia. *Journal of Applied Volcanology*, 12(1), 1–20. doi: 10.1186/s13617-023-00129-2

Ashari, A. (2018). Geomorphology Of The Southern Flank Of Merapi Volcano In Relation To The Potential Hazards And Natural Resources: A Review. *Geomedia: Majalah Ilmiah dan Informasi Kegeografian*, 15(2). doi: 10.21831/gm.v15i2.19556

Azizah, V., Listyo, D., & Irawan, Y. (2023). *Deteksi Perubahan Jalur Lahar di Curah Lengkong Pasca Erupsi Gunungapi Semeru 2021 Menggunakan Google Earth Engine*. 7(1), 70–93.

Bachri, S., Shrestha, R. P., Sumarmi, Irawan, L. Y., Masruroh, H., Prastiwi, M. R. H., Billah, E. N., Putri, N. R. C., Hakiki, A. R. R., & Hidiyah, T. M. (2024). Land use change simulation model using a land change modeler in anticipation of the impact of the Semeru volcano eruption disaster in Indonesia. *Environmental Challenges*, 14, 100862. doi: 10.1016/J.ENVC.2024.100862

Bachri, S., Stötter, J., Monreal, M., & Sartohadi, J. (2015). The calamity of eruptions, or an eruption of benefits? Mt. Bromo human-volcano system a case study of an open-risk perception. *Natural Hazards and Earth System Sciences*, 15(2), 277–290. doi: 10.5194/nhess-15-277-2015

Barbosa de Souza, K., Rosa dos Santos, A., Macedo Pezzopane, J. E., Machado Dias, H., Ferrari, J. L., Machado de Oliveira Peluzio, T., Toledo, J. V., Freire Carvalho, R. de C., Rizzo Moreira, T., & França Araújo, E. (2023). Modeling dynamics in land use and land cover and its future projection for the amazon biome. *Forests*, 14(7), 1281.

Baxter, P. J., Jenkins, S., Seswandhana, R., Komorowski, J.-C., Dunn, K., Purser, D., Voight, B., & Shelley, I. (2017). Human survival in volcanic eruptions: Thermal injuries in pyroclastic surges, their causes, prognosis and emergency management. *Burns*, 43(5), 1051–1069. doi: 10.1016/j.burns.2017.01.025

Bermana, I. (2006). Klasifikasi geomorfologi untuk pemetaan geologi yang telah dibakukan. *Bulletin of Scientific Contribution*, 4(2), 161–173.

Budiyanto, G. (2020). Land use planning for disaster-prone areas in southern region of mount Merapi. *AGRIVITA Journal of Agricultural Science*, *43*(1), 1–12.

Cando-Jácome, M., & Martínez-Graña, A. (2019). Determination of primary and secondary lahar flow paths of the Fuego Volcano (Guatemala) using morphometric parameters. *Remote Sensing*, 11(6). doi: 10.3390/rs11060727

Dammag, A. Q., Jian, D., Cong, G., Derhem, B. Q., & Latif, H. Z. (2023). Predicting spatio-temporal land use/land cover changes and their drivers forces based on a cellular automated Markov model in Ibb City, Yemen. *Geocarto International*, 38(1), 2268059.

Darmawan, K., Hani'ah, H., & Suprayogi, A. (2017). Analisis Tingkat Kerawanan Banjir di Kabupaten Sampang Menggunakan Metode Overlay dengan Scoring Berbasis Sistem Informasi Geografis. *Jurnal Geodesi Undip*, 6(1), 31–40.

Dharmawan, I. W. S., & Pratiwi. (2023). Implementation of forest-land rehabilitation to support the enhancement of carbon stock on Indonesia's FOLU net sink 2030 strategy. *IOP Conference Series: Earth and Environmental Science*, 1180(1), 12010.

Epie, W. N., & Hull, S. (2025). Land use and land cover change detection and prediction in the cross-Sanaga-Bioko coastal forest for sustainable forest management. *African Geographical Review*, 1–26.

ESDM. (2024). *Beberapa Gunung Api Alami Peningkatan Aktivitas Vulkanik, Badan Geologi Minta Masyarakat Tetap Waspada*. Retrieved From https://esdm.go.id/en/media-center/news-archives/beberapa-gunung-api-alami-peningkatan-aktivitas-vulkanik-badan-geologi-minta-masyarakat-tetap-waspada#:~:text=Pusat Vulkanologi dan Mitigasi Bencana Geologi (PVMBG),beberapa gunung api di Indonesia mengalami peni

Feizizadeh, B., Omarzadeh, D., Kazemi Garajeh, M., Lakes, T., & Blaschke, T. (2023). Machine learning data-driven approaches for land use/cover mapping and trend analysis using Google Earth Engine. *Journal of Environmental Planning and Management*, 66(3), 665–697. doi: 10.1080/09640568.2021.2001317

Gontier, M., Mörtberg, U., & Balfors, B. (2010). Comparing GIS-based habitat models for applications in EIA and SEA. *Environmental Impact Assessment Review*, 30(1), 8–18. doi: 10.1016/j.eiar.2009.05.003

Hadmoko, D. S., de Belizal, E., Mutaqin, B. W., Dipayana, G. A., Marfai, M. A., Lavigne, F., Sartohadi, J., Worosuprojo, S., Starheim, C. C. A., & Gomez, C. (2018). Post-eruptive lahars at Kali Putih following the 2010 eruption of Merapi volcano, Indonesia: occurrences and impacts. *Natural Hazards*, 94(1), 419–444. doi: 10.1007/s11069-018-3396-7

Harist, M. C., Afif, H. A., Putri, D. N., & Shidiq, I. P. A. (2018). GIS modelling based on slope and morphology for landslide potential area in Wonosobo, Central Java. *MATEC Web of Conferences*, 229, 03004. doi: 10.1051/matecconf/201822903004

Hasan, S., Shi, W., Zhu, X., Abbas, S., & Khan, H. U. A. (2020). Future simulation of land use changes in rapidly urbanizing South China based on land change modeler and remote sensing data. *Sustainability (Switzerland)*, 12(11). doi: 10.3390/su12114350

Hasnaini, H., Yuwono, Y., & Deviantari, U. W. (2024). Pemetaan Kesesuaian Pengembangan Objek Wisata Waduk Selorejo Berdasarkan Kondisi Fisik Lapangan. *Jurnal Teknik ITS*, 13(1). doi: 10.12962/j23373539.v13i1.127293

Iswari, M. Y., & Anggraini, K. (2018). Demnas: Model Digital Ketinggian Nasional Untuk Aplikasi Kepesisiran. *Oseana*, 43(4). doi: 10.14203/oseana.2018.Vol.43No.4.2

Kadam, S., Patil, S., Sawant, K., Jamdade, S., Gadilkar, A., Ohri, C., Rathi, N., & Gujar, J. (2025). Comparative Analysis of CART and Random Forest Classifiers for LULC Mapping: A Case Study of Brahmani-Baitarani River Basin, India. *Nature Environment and Pollution Technology*, 24(4), 1–13.

Kassouk, Z., Thouret, J.-C., Gupta, A., Solikhin, A., & Liew, S. C. (2014). Object-oriented classification of a high-spatial resolution SPOT5 image for mapping geology and landforms of active volcanoes: Semeru case study, Indonesia. *Geomorphology*, 221, 18–33. doi: 10.1016/j.geomorph.2014.04.022

Kaur, H., Tyagi, S., Mehta, M., & Singh, D. (2023). Time series (2001/2002–2021) analysis of Earth observation data using Google Earth Engine (GEE) for detecting changes in land use land cover (LULC) with specific reference to forest cover in East Godavari Region, Andhra Pradesh, India. *Journal of Earth System Science*, 132(2), 86.

Krisanti, M. W. W., Paripurno, E. T., Nugroho, A. R. B., Maharani, Y. N., & Prasetya, J. D. (2024). Community-Based land use models for sustainable livelihoods in Merapi Volcano disaster prone areas III in Sleman Regency. *IOP Conference Series: Earth and Environmental Science*, 1314(1). doi: 10.1088/1755-1315/1314/1/012048

Kristianto, Nugraha Kartadinata, M., & Kamil Syahbana, D. (2024). Contingency Planning for Tourism Development in Volcanic Disaster-Prone Areas in Indonesia. *IOP Conference Series: Earth and Environmental Science*, 1424(1), 12031.

Lessy, M. R., Lassa, J., & Zander, K. K. (2024). Understanding Multi-Hazard Interactions and Impacts on Small-Island Communities: Insights from the Active Volcano Island of Ternate, Indonesia. *Sustainability*, 16(16), 6894.

Leta, M. K., Demissie, T. A., & Tränckner, J. (2021). Modeling and prediction of land use land cover change dynamics based on land change modeler (Lcm) in nashe watershed, upper blue nile basin, Ethiopia. *Sustainability*, 13(7), 3740.

Malawani, M. N., Lavigne, F., Gomez, C., Mutaqin, B. W., & Hadmoko, D. S. (2021). Review of local and global impacts of volcanic eruptions and disaster management practices: The Indonesian example. In *Geosciences (Switzerland)*, 11(3), bll 1–18. doi: 10.3390/geosciences11030109

Meredith, E. S., Teng, R. X. N., Jenkins, S. F., Hayes, J. L., Biass, S., Tennant, E., & Handley, H. (2025). Global trends of city exposure to volcanic hazards. *EGU General Assembly Conference Abstracts*, EGU25-6959.

Mishra, V. N., Rai, P. K., Prasad, R., Punia, M., & Nistor, M.-M. (2018). Prediction of spatio-temporal land use/land cover dynamics in rapidly developing Varanasi district of Uttar Pradesh, India, using geospatial approach: a comparison of hybrid models. *Applied Geomatics*, 10(3), 257–276. doi: 10.1007/s12518-018-0223-5

Muthohar, I., Balijepalli, C., & Priyanto, S. (2020). Analysing vulnerability of road network and guiding evacuees to sheltered areas: Case study of Mt Merapi, Central Java, Indonesia. *Case studies on transport policy*, 8(4), 1329–1340.

Mutiarni, Y. S., Nakamura, H., & Bhattacharya, Y. (2022). The Resilience Community: Strengthening People-Centered Disaster Risk Reduction in the Merapi Volcano Community, Java, Indonesia. *Sustainability (Switzerland)*, 14(4). doi: 10.3390/su14042215

Nugraha, A. L., Firdaus, H. S., & Haeriah, S. (2019). Analysis of risk assessment of Mount Merapi eruption in settlement area of Sleman Regency. *IOP conference series: earth and environmental science*, 313(1), 12003.

Nugroho, S. P., Tarigan, S. D., & Hidayat, Y. (2018). Analisis Perubahan Penggunaan Lahan Dan Debit Aliran Di Sub Das Cicatih. *Jurnal Pengelolaan Sumberdaya Alam dan Lingkungan (Journal of Natural Resources and Environmental Management)*, *8*(2), 258–263. doi: 10.29244/jpsl.8.2.258-263

Ojelabi, O. K., Lawin, A. E., Amichiatchi, N. J., & Oluwasemire, K. O. (2025). Impacts of anthropogenic activities on land use land cover change dynamics in the Ogun River Basin, Nigeria. *Journal of Water and Climate Change*, 16(1), 174–188.

Ouchra, H., Belangour, A., & Erraissi, A. (2023). Exploring google earth engine platform for satellite image classification using machine learning algorithms. *The Proceedings of the International Conference on Smart City Applications*, 271–280.

Pande, C. B., Diwate, P., Orimoloye, I. R., Sidek, L. M., Pratap Mishra, A., Moharir, K. N., Pal, S. C., Alshehri, F., & Tolche, A. D. (2024). Impact of land use/land cover changes on evapotranspiration and model accuracy using Google Earth engine and classification and regression tree modeling. *Geomatics, Natural Hazards and Risk*, 15(1). doi: 10.1080/19475705.2023.2290350

Puspita, B. D., & Sudaryatno. (2013). Estimasi Sedimen Lahar Dingin di Sebagian Kali Gendol Gunung Merapi Menggunakan FUFK dan Lidar. *Jurnal Bumi Indonesia*, 2(3), 92–98.

Rani, M., & Khotimah, N. (2021). Disaster Risk Analysis of Merapi Volcano Eruption in Cangkringan District Sleman Regency. *IOP Conference Series: Earth and Environmental Science*, 884(1). doi: 10.1088/1755-1315/884/1/012051

Rasidi, Ghufron, A., Wangid, M. N., & Istiningsih, G. (2023). Volcanic Eruption Disaster Response: A Model for Assisting Children in Learning in Refugee Camps in Indonesia. *Proceedings of the 3rd Borobudur International*

Symposium on Humanities and Social Science 2021 (BIS-HSS 2021), 954–965. doi: 10.2991/978-2-494069-49-7_161

Ridwan, F., Ardiansyah, M., & Gandasasmita, K. (2017). Pemodelan Perubahan Penutupan/Penggunaan Lahan Dengan Pendekatan Artificial Neural Networkdan Logistic Regression(Studi Kasus: Das Citarum, Jawa Barat). *Buletin Tanah dan Lahan*, 1(1), 30–36.

Rimba, A. B., Atmaja, T., Mohan, G., Chapagain, S. K., Arumansawang, A., Payus, C., & Fukushi, K. (2020). Identifying Land Use and Land Cover (LULC) Change From 2000 bo 2025 Driven By Tourism Growth: A Study Case In Bali. *The International Archives of the Photogrammetry, Remote Sensing and Spatial Information Sciences*, *XLIII-B3-2020*, 1621–1627. doi: 10.5194/isprs-archives-XLIII-B3-2020-1621-2020

Sabiri, B., El Asri, B., & Rhanoui, M. (2022). Efficient deep neural network training techniques for overfitting avoidance. *International Conference on Enterprise Information Systems*, 198–221.

Sajan, B., Mishra, V. N., Kanga, S., Meraj, G., Singh, S. K., & Kumar, P. (2022). Cellular automata-based artificial neural network model for assessing past, present, and future land use/land cover dynamics. *Agronomy*, 12(11), 2772.

Santosa, L. W., & Sutikno, S. (2006). Geomorphological approach for regional zoning in the Merapi volcanic area. *Indonesian Journal of Geography*, 38(1).

Sejati, S. P., & Neritarani, R. (2024). The impact of land use change on groundwater depth in the groundwater transition zone of Merapi Volcano, Yogyakarta, Indonesia. *The Indonesian Journal of Geography*, 56(1), 96–115.

Septikasari, Z., & Ayriza, Y. (2018). Strategi Integrasi Pendidikan Kebencanaan Dalam Optimalisasi Ketahanan Masyarakat Menghadapi Bencana Erupsi Gunung Merapi. *Jurnal Ketahanan Nasional*, 24(1). doi: 10.22146/jkn.33142

Shang, M., & Luo, J. (2021). The tapio decoupling principle and key strategies for changing factors of chinese urban carbon footprint based on cloud computing. *International Journal of Environmental Research and Public Health*, 18(4), 1–17. doi: 10.3390/ijerph18042101

Solikhin, A., Thouret, J.-C., Liew, S. C., Gupta, A., Sayudi, D. S., Oehler, J.-F., & Kassouk, Z. (2015). High-spatial-resolution imagery helps map deposits of the large (VEI 4) 2010 Merapi Volcano eruption and their impact. *Bulletin of volcanology*, 77(3), 20.

Subiyanto, S., Sukmono, A., Bashit, N., & Amarrohman, F. J. (2019). The use of a MLP neural network for analysis and aodeling of land use changes with variations variable of physical and economic social. *IOP Conference Series: Earth and Environmental Science*, 389(1), 12029.

Sun, J., Jiang, N., Sun, G., & Huang, W. (2023). Analysis of CART algorithms in data mining. *2023 2nd International Conference on Machine Learning, Cloud Computing and Intelligent Mining (MLCCIM)*, 548–553.

Tekla, T. B., Galato, S. D., Tussie, G. D., & Zeleke, G. A. (n.d.). Analysis of Land Use and Land Cover Trends Using Google Earth Engine and Machine Learning Algorithms: The Case of Welmel Watershed, Southeastern Ethiopia. *Southeastern Ethiopia*.

Thi Anh Thu, T., Thi An, T., Le Tan Dat, N., & Kim Loi, N. (2024). Utilization of Landsat Imagery and Google Earth Engine to Analyze the Urban Growth Dynamics in Thuan An City, Binh Duong Province. *IOP Conference Series: Earth and Environmental Science*, 1345(1), 12005.

Thouret, J.-C., Lavigne, F., Kelfoun, K., & Bronto, S. (2000). Toward a revised hazard assessment at Merapi volcano, Central Java. *Journal of Volcanology and Geothermal Research*, 100(1–4), 479–502. doi: 10.1016/S0377-0273(00)00152-9

Thouret, J. C., Wavelet, E., Taillandier, M., Tjahjono, B., Jenkins, S. F., Azzaoui, N., & Santoni, O. (2022). Defining population socio-economic characteristics, hazard knowledge and risk perception: The adaptive capacity to persistent volcanic threats from Semeru, Indonesia. *International Journal of Disaster Risk Reduction*, 77. doi: 10.1016/j.ijdrr.2022.103064

Triwahyuni, L. (2017). Sobirin, and Ratna Saraswati,"Analisis Spasial Wilayah Potensi Longsor dengan Metode SINMAP dan SMORPH di Kabupaten Kulon Progo, Daerah Istimewa Yogyakarta". *Industrial Research Workshop and National Seminar*, 69–76.

Walter, T. R., Wang, R., Zimmer, M., Grosser, H., Lühr, B., & Ratdomopurbo, A. (2007). Volcanic activity influenced by tectonic earthquakes: Static and dynamic stress triggering at Mt. Merapi. *Geophysical Research Letters*, 34(5). doi: 10.1029/2006GL028710

Widiatmoko, N., Tarigan, S. D., & Wahjunie, E. D. (2020). Analisis Respons Hidrologi untuk Mendukung Perencanaan Pengelolaan Sub-DAS Opak Hulu, Daerah Istimewa Yogyakarta. *Jurnal Ilmu Pertanian Indonesia*, 25(4), 503–514. doi: 10.18343/10.18343/jipi.25.4.503

Widodo, E., Alamsyah, E., Rifa'atussa'adah, N., & Hastuti, H. (2024). Kondisi Jalur Evakuasi Gunungapi Merapi (Studi Kasus Di Kabupaten Magelang). *Geomedia: Majalah Ilmiah dan Informasi Kegeografian*, 22(1). hdoi: 10.21831/gm.v22i1.52336

Yu, X., Xiao, J., Huang, K., Li, Y., Lin, Y., Qi, G., Liu, T., & Ren, P. (2023). Simulation of land use based on multiple models in the Western Sichuan Plateau. *Remote Sensing*, 15(14), 3629.

Zuidam, R. A. van. (1985). Aerial photo-interpretation in terrain analysis and geomorphologic mapping. *ITC, Smits Publ., Enschede, The Hague*.